

# HunyuanPortrait: Implicit Condition Control for Enhanced Portrait Animation

Zunnan Xu<sup>1,2\*</sup>, Zhentao Yu<sup>2</sup>, Zixiang Zhou<sup>2</sup>, Jun Zhou<sup>3\*</sup>, Xiaoyu Jin<sup>1\*</sup>, Fa-ting Hong<sup>4\*</sup>,  
Xiaozhong Ji<sup>2</sup>, Junwei Zhu<sup>2</sup>, Chengfei Cai<sup>2</sup>, Shiyu Tang<sup>2</sup>, Qin Lin<sup>2</sup>, Xiu Li<sup>1†</sup>, Qinling Lu<sup>2†</sup>  
<sup>1</sup>Tsinghua University <sup>2</sup>Hunyuan, Tencent <sup>3</sup>Sun Yat-Sen University <sup>4</sup>HKUST

## Abstract

We introduce *HunyuanPortrait*, a diffusion-based condition control method that employs implicit representations for highly controllable and lifelike portrait animation. Given a single portrait image as an appearance reference and video clips as driving templates, *HunyuanPortrait* can animate the character in the reference image by the facial expression and head pose of the driving videos. In our framework, we utilize pre-trained encoders to achieve the decoupling of portrait motion information and identity in videos. To do so, implicit representation is adopted to encode motion information and is employed as control signals in the animation phase. By leveraging the power of stable video diffusion as the main building block, we carefully design adapter layers to inject control signals into the denoising unet through attention mechanisms. These bring spatial richness of details and temporal consistency. *HunyuanPortrait* also exhibits strong generalization performance, which can effectively disentangle appearance and motion under different image styles. Our framework outperforms existing methods, demonstrating superior temporal consistency and controllability. Our project is available at [HunyuanPortrait](#).

## 1. Introduction

In this paper, we aim to animate a single static image into a lifelike video using control signals in implicit representations derived from driving videos. As shown in Figure 1, our primary focus is not only on the high controllability of digital portraits but also on the strong consistency of the characters and background in the reference image.

Portrait animation has been widely applied in fields such as human-computer interaction [12, 58], virtual reality, and the crafting of digital avatars for the gaming and multimedia industries [29–31]. Previous works [4, 7, 64] develop usable portrait animation models utilizing Generative Adversarial Networks (GANs) [11] based on raw video inputs. However, these approaches exhibit limitations in terms of gener-

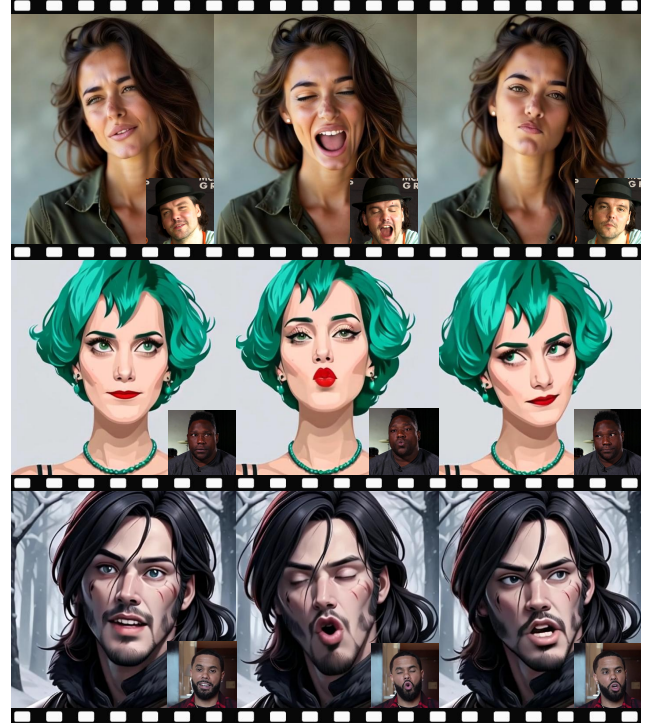


Figure 1. Our framework employs implicit condition control to generate portrait animations, demonstrating robust generalization performance with high-fidelity facial dynamics and vivid head poses during cross-reenactment. The animated portraits remain unaffected by variations in facial shape and the spatial position of the driving videos, demonstrating strong identity consistency.

alization. Given the variability of facial structures and the complexities of facial movements, these methods often face challenges such as artifacts and insufficient control over facial expressions. This is particularly evident when there is a substantial difference in facial shape between the driving video and the source image, resulting in significant issues with facial artifacts and motion distortion. These early methods often produce results with background jitter and blurred portraits during cross-reenactment [37, 43].

The advancement of diffusion models has led to a significant focus in recent methodologies [3, 50] on the fine-tuning

\*Work done during the internship at Tencent.

†Corresponding author.

of image-level diffusion models [41] through the incorporation of motion modules [15], thereby facilitating the generation of video content. These methods effectively address the issues associated with GAN-based approaches in managing complex backgrounds and enhancing generalization. However, even with the incorporation of motion modules, these methods are susceptible to defects during the generation stage (e.g., temporal smoothness and flexibility to different frame rates). This vulnerability arises from the absence of motion pre-training in the underlying models during the pre-training phase. Additionally, these methods remain constrained to the explicit control of facial expressions. The effectiveness of these methods, which depend on explicit keypoints to control facial expressions, not only results in the loss of intricate details but also significantly relies on the accuracy of the landmark extraction techniques employed. Furthermore, as a result of the variability in facial shapes, these methods are limited by post-processing alignment strategies and often face challenges in adapting to diverse facial geometries, which can lead to inaccurate facial control and insufficient preservation of identity in the visual effects of videos. Due to the human eye’s sensitivity to subtle facial changes [47], it is crucial to preserve the fidelity of facial details and the smoothness of the videos.

Therefore, we propose an implicit conditional control model to tackle the challenges posed by diverse facial geometries and intricate expression details. We utilize stable video diffusion as the foundational model and integrate identity and motion information through appearance and motion attention. This approach eliminates the need to fine-tune the image diffusion model and to train the motion module separately. Firstly, we coarsely decouple the identity information from the motion information in the original video by using a pre-trained motion encoder [9]. Considering that this pre-trained encoder has not completely decoupled identity from motion information, we further implement enhanced training strategies and improved network architectures to strengthen the control of motion features and the separation of portrait identities. For the adaptation of temporal modeling tasks in video generation using diffusion models, along with the complementary contextual information present between different frames, we propose the incorporation of a motion memory bank to enhance the implicit representation of motion features. Due to the substantial variations in the degree of blur and pixel distortion in video frames at different levels of motion intensity, we propose an intensity-aware motion encoder. This encoder aims to improve the capacity of decoupled motion features to capture intricate details. Additionally, in order to achieve consistent modeling of portrait identity and background areas in videos, we combined ArcFace [6] with the DiNOv2 [38] backbone to develop an enhanced appearance encoder. To preserve the pre-training knowledge of both models, we

froze their original parameters and proposed an ID-aware Multi-scale adapter (IMAdapter). This approach achieves high-fidelity modeling of the intricate details in portraits. Our main contributions can be summarized as follows:

- We propose the first implicit condition animation framework based on stable video diffusion, which significantly improves temporal consistency and achieves high fidelity and precise control for portrait animation.
- We develop a series of strategies to enhance identity consistency and improve the accuracy of portrait motion, including data augmentation, enhanced training and inference strategies, and improved network architecture.
- Experiments demonstrate the effectiveness of our proposed method, which achieves state-of-the-art performance in both subjective and objective metrics.

## 2. Related Work

Human portrait animation aims to bring a still image to life by utilizing a driving source, such as a sequence of facial landmarks or frames that contain the head of the portrait. Recent advancements in the field of neural avatars can be divided into two subcategories: non-diffusion-based and diffusion-based methods. Non-diffusion-based methods [14, 18, 19, 27, 44, 51, 57, 64, 68] are renowned for their ability to achieve realistic facial animations and fidelity to motion. Many works employed predetermined motion representations that are popular in the literature, such as blend-shapes from 3D Morphable Models (3DMM) [7, 21, 23, 36, 46, 62, 63]. However, these works often display significant artifacts when there is a large disparity between the driving portrait and the source image. Due to the use of a warping-based strategy, these methods are also ineffective at capturing videos with significant head and body movements. With the development of diffusion models [26], recent methods [13, 53, 55, 59] achieve human portrait animation by fine-tuning the stable diffusion model [41]. Several studies have investigated the generation of facial expressions through explicit keypoint control [3, 50, 69]. This method shows great promise for enhancing the quality of generated videos and enables precise control of facial expressions through the extraction of facial landmarks. However, given the diversity of facial geometries, there are notable differences in the distribution of facial keypoints among individuals. The alignment processes used in these methods often struggle to manage boundary cases effectively, resulting in identification offsets due to inaccurate alignment. In addition, the reliance on image-based generative models and separately trained motion modules to achieve temporal consistency results in shortcomings related to temporal smoothness. In the pursuit of improved temporal continuity, pioneering work [22, 28, 39, 66] has employed stable video diffusion models to construct end-to-end diffusion models for human video generation. However, these methods are pri-

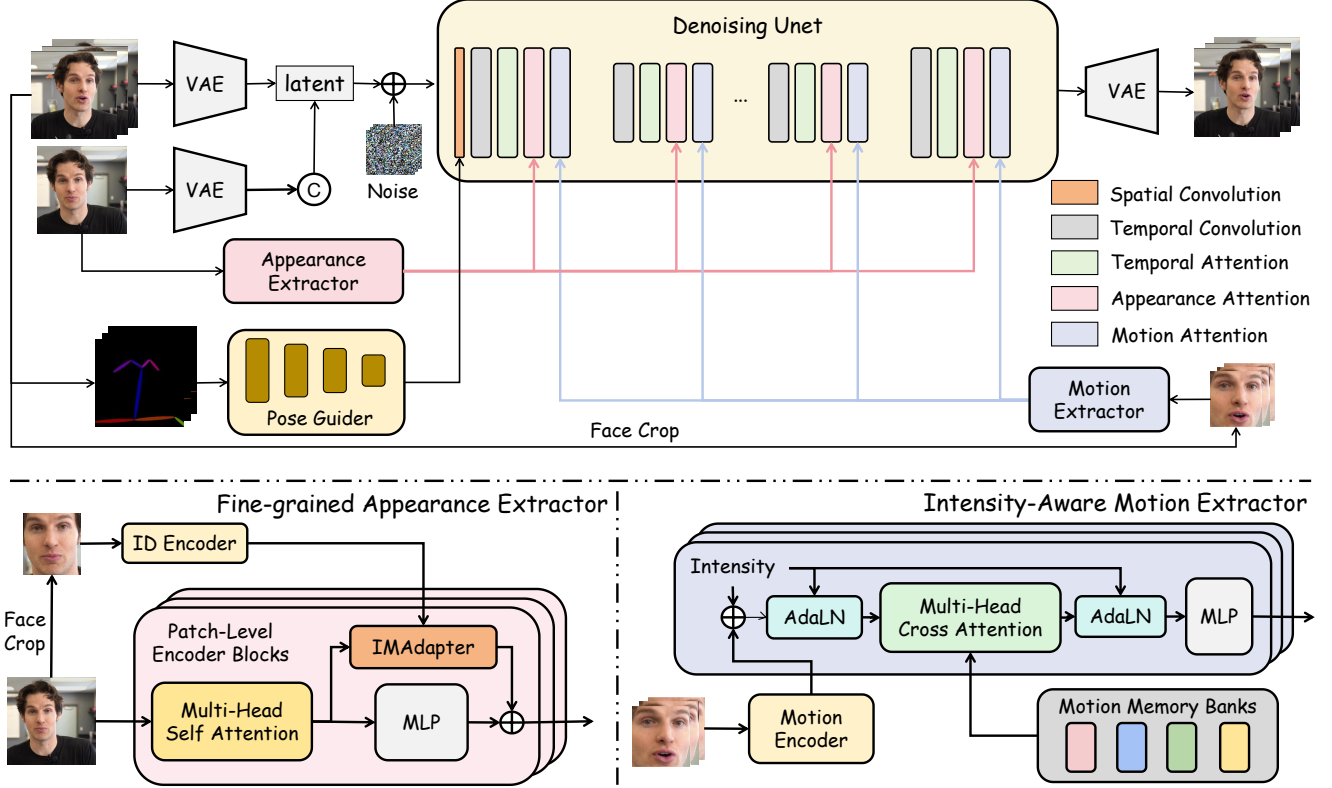


Figure 2. Our framework utilizes implicit representation to encode motion information as control signals. By harnessing the capabilities of stable video diffusion as the primary building block, we have meticulously designed a fine-grained appearance extractor to maintain the identity of the portrait, along with an intensity-aware motion extractor to capture intricate facial dynamics.

marily designed for full-body movements and do not take into account the preservation of facial identity or the diversity of human facial geometries. As a result, they often lead to significant alterations in the identity of the generated face. Additionally, these methods lack the ability to control subtle facial dynamics, which limits their application in generating portraits that incorporate speech content and facial expressions. In this study, we investigate the strategy of adapting to various face shapes through implicit representations of expression descriptors and achieving capture of facial dynamics. Our method surpasses previous approaches in terms of temporal consistency and generalization ability.

### 3. Methodology

#### 3.1. Preliminaries

**Diffusion Model.** Our framework is built upon diffusion model, as introduced in [41]. The model is designed to facilitate efficient and stable training by conducting the diffusion and denoising processes within a latent space, rather than directly in the image space. The Variational Autoencoder (VAE), as proposed in [24], plays a pivotal role in this process by mapping images from the RGB color space into

a latent space. This transformation enables the diffusion process to be directed by textual embeddings.

The process begins with the VAE model, which projects images into latent embeddings. This model comprises two key components: an encoder  $\mathcal{E}$  and a decoder  $\mathcal{D}$ . The encoder  $\mathcal{E}$  compresses the pixel space image  $x$  into a latent representation  $z = \mathcal{E}(x)$ , while the decoder  $\mathcal{D}$  reconstructs it back into an image space, aiming for  $\mathcal{D}(z) \approx x$ . Subsequently, a UNet-based architecture [42] is employed for learning the reverse denoising process within the latent space. This network integrates attention mechanisms through Transformer Blocks. The cross-attention mechanism ensures that the textual prompt is effectively integrated throughout the process. The overall training objective for the UNet can be articulated as follows:

$$\mathcal{L} = \mathbb{E}_{t, z, \epsilon} [\|\epsilon - \epsilon_{\theta}(\sqrt{\alpha_t}z + \sqrt{1 - \alpha_t}\epsilon, c, t)\|^2], \quad (1)$$

where  $z$  denotes the latent embedding of the training sample.  $\epsilon_{\theta}$  and  $\epsilon$  represent the predicted noise by the diffusion model and the ground truth noise at the corresponding timestep  $t$ , respectively.  $c$  is the condition embedding, and the coefficient  $\alpha_t$  remains consistent with that employed in diffusion models.

### 3.2. Overall framework

As illustrated in Figure 2, building upon stable video diffusion [1], our method is designed with two core components for generating portrait videos: the appearance extractor and the motion extractor. For the detailed appearance modeling of the portrait, we integrate the appearance encoder to manage the subject’s identity and background in the generated video. We carefully design an ID-aware multi-scale adapter based on the Arcface encoder [6] and DiNOv2 [38] backbone to enhance visual appearance representation. For the motion extractor, we emphasize the enhancement of the implicit representation of facial dynamics. By utilizing the pre-trained motion encoder [8], we further optimize it by taking into account the intensity and the temporal continuity of motions. This involved the introduction of motion memory banks and an intensity-aware motion encoder to enhance the perception of motion intensity and refine features. These representations are conditionally integrated into the denoising U-Net through attention mechanisms. Our framework also integrates a spatial conditioning signal to ensure the stability of regions beyond the face. By utilizing these features, we generate latent features using a denoising UNet and subsequently produce video through VAEs.

### 3.3. Intensity-Aware Motion Extractor

For portrait motion modeling, we concentrate on identity-agnostic portrait animation by utilizing an implicit representation of expression descriptors derived from raw videos, which capture a diverse array of facial dynamics (e.g., lip-sync, micro-expressions, eye gaze, and blinking). This approach differs from existing diffusion-based methods that typically employ explicit landmarks for facial expression representation [34, 53]. Considering that the fidelity of facial motion capture is often compromised by extraneous factors—such as variations in facial shape and background noise that can distort essential motion signals—we crop the central area of the face to focus on the regions most indicative of motion dynamics. The boundary is defined as the area between the eyebrows and the bottom of the mouth. This approach allows us to isolate facial movements and enhance the signal-to-noise ratio. The cropped pixels from driving videos are subsequently utilized as inputs for the pre-trained motion encoder [8] to extract a coarse implicit conditioning signal. Since motion intensity varies and exerts distinct influences on the generated pixels, we introduce an Intensity-Aware Motion Encoder into our framework. This addition enhances the coarse motion features from the motion encoder by adapting to the varying intensities of motion. The intensity is estimated by two dimensions: the degree of distortion in facial expressions and the overall amplitude of head movement. Considering that the expression and head pose intensity rely on landmark positioning and their relative differences, we propose a calcu-

lation method for these variances using landmarks and normalization, which can be formulated as below:

$$\begin{aligned} e_{k,j} &= l_{k,j} - l_{k,c}, k \in [1, n], j \in [1, m] \\ s &= \sqrt{(l_{1,\max} - l_{1,\min})^2}, \end{aligned} \quad (2)$$

where  $l_{k,j}$  denotes the  $j$ -th landmark point in the  $k$ -th frame and  $l_{k,c}$  denotes the center of the landmark point (e.g., nose tip).  $n$  and  $m$  denote the numbers of frames and points.  $s$  represents the face scale derived from the first frame of the landmarks. We further calculate the intensity of expressions  $I_e$  and the head poses  $I_h$  using the formulation below:

$$\begin{aligned} I_e &= \frac{1}{n \cdot s} \sum_{k=1}^n \sqrt{\frac{1}{m} \sum_{j=1}^m (e_{k,j} - \frac{1}{n} \sum_{k=1}^n e_{k,j})^2}, \\ I_h &= \frac{1}{s} \sqrt{\frac{1}{n} \sum_{k=1}^n (l_{k,c} - \frac{1}{n} \sum_{k=1}^n l_{k,c})^2}. \end{aligned} \quad (3)$$

Considering the issue of accuracy in landmark detection, we discretize the calculated continuous values by dividing the intensity into  $d$  discrete levels based on the range of values. We set  $d$  to 64 and then map these discrete values using embeddings  $\mathcal{D}$  to their corresponding intensity feature vectors  $E_s = \text{Concat}[\mathcal{D}(I_e), \mathcal{D}(I_h)]$ , and concatenate them along the channel dimension to adjust the feature space in response to the dynamic range of motion intensity. In light of the fact that the sequence of motion features is derived from pixel extraction and exhibits a lack of continuity across different contexts, we propose the motion memory bank to improve the context-awareness and temporal modeling capabilities of motion features, which can be formulated as below:

$$\begin{aligned} \hat{f}_m &= \text{AdaLN}(F_m + E_s, E_s), \\ \bar{f}_m &= \text{MHCA}(\hat{m}, \hat{f}_m, \hat{f}_m), \\ \bar{f}_m &= \text{AdaLN}(\bar{f}_m, E_s), \\ \bar{f}_m &= \text{MLP}(\bar{f}_m), \end{aligned} \quad (4)$$

where  $F_m$  denotes the features extracted by the pre-trained motion encoder, and  $\hat{m}$  signifies the query features from the motion memory bank, with  $\hat{f}_m$  being utilized as the key and value features. The MHCA denotes multi-head cross-attention [49] and the AdaLN denotes adaptive layer normalization [56]. The learnable memories are designed to supplement contextual information, enriching motion features rather than generating new motions. This helps the model capture pixel correlation between different frames, alleviating blurring when some facial parts undergo deformation. The refined motion features are incorporated into the denoising U-Net using cross-attention mechanisms [61].



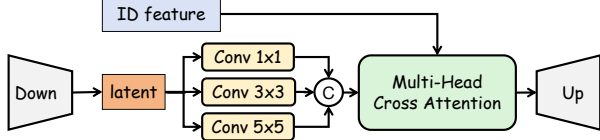


Figure 3. The illustration of our ID-aware Multi-scale Adapter (IMAdapter). Here, © represents the operation of concatenating features along the channel dimension.

### 3.4. Fine-grained Appearance Extractor

To achieve appearance control, which encompasses both portrait identity information and background details, we propose an appearance extractor that creates a fine-grained representation of the animated portrait and background. Existing video diffusion models often struggle with identity consistency [39, 66], which results in deficiencies in the method’s capacity to generate portraits. Due to the human eye’s sensitivity to subtle facial changes, visual artifacts can lead to inaccurate facial details and insufficient preservation of identity in the generated videos. Therefore, we adopt a patch-level image encoder [38] as the backbone of the appearance encoder and introduce an ID-aware multi-scale adapter (IMAdapter) to enhance the model’s ID consistency capabilities. To process the entire image, we first extract information related to clothing and background elements of the portrait. For the enhancement of consistency, as illustrated in Figure 2, we utilize the ID encoder to extract identity-related features. We further propose extracting multi-scale, fine-grained identity features using adapters.

As illustrated in Figure 3, we first use the linear projection to downsample the visual features. The low-rank features are subsequently fed into convolutional modules at multiple scales, along with a cross-attention mechanism, which captures ID-aware fine-grained details for the preservation of visual identity. The cross-modal features are then linearly projected back to the original dimensions to be merged with patch-level features:

$$\begin{aligned}
 \hat{f}_a &= f_a \mathbf{W}_{down}^v, \\
 \hat{f}_c &= \text{MConv}(\hat{f}_a), \\
 \bar{f}_a &= \text{MHCA}(f_{id}, \hat{f}_c, \hat{f}_c), \\
 f_a &= f_a + \bar{f}_a \mathbf{W}_{up}^v,
 \end{aligned} \tag{5}$$

where  $f_{id}$  represents the ID features, which are utilized as the query features, while  $\hat{f}_c$  serves as the key and value features. MConv signifies the multiple convolutions that process appearance features  $f_a$  in parallel and concatenate them along the channel dimension. During the training phase, the sampling of ID information comes from a random frame in the video sequence; in the inference stage, it comes from the reference image.

### 3.5. Training and Inference Strategies

For adaptation to various anime styles, we utilize AnimeGANv3 [32] to perform style conversion on the dataset. This allows the model to adjust to different styles of driving videos and source images. Instead of directly training models with AnimeGANv3, we employ its style transfer capability to convert facial portrait datasets into anime-stylized representations. These transformed data samples are then integrated into our training dataset for enhanced feature learning. To mitigate the impact of skin color and other color-related information on facial movements, we employ color jittering to augment the data for the facial cropping input of the motion encoder. For maintaining the stability of the regions beyond the face in the generated video, we utilize DWPose [60] as an additional spatial conditioning signal. Specifically, we employ the pose-guided network [20] to achieve spatial control condition mapping. We further incorporate spatial conditional control into the latent features of the first spatial convolutional layer in U-Net through addition. To simulate scenarios in which certain skeletons from the driving video are absent compared to those in the source image during the inference stage, we implement an augmentation strategy [50] for the pose sequence during training. This strategy randomly removes certain edges throughout the training process to improve the stability of spatial control. This mitigates the effects of detector accuracy limitations on detector-based control conditions and offers flexible control capability. During inference, considering that there are differences in the body shape and spatial position of bones between the source image and the driving video, we first translate the position based on the offset of the center point of the face (e.g., the position of the nose tip) and scale it according to the length ratio of the skeletons. We find that the key points of the eyes can lead to subtle variations in face shape. Therefore, in the setting of cross reenactment, we do not utilize the key points and corresponding edges of the eyes.

## 4. Experiments

### 4.1. Experiments Setting

We train our model using HDTF [67], VFHQ [54], VoxCeleb2 [5], CelebV-HQ [70], and our own collected dataset. This collected dataset comprises monocular camera recordings showcasing 20 hours of authentic human video footage obtained from 200 subjects. The recordings were captured in both indoor and outdoor environments. During the training process, all of the images and videos are resized to  $512 \times 512$ . For the optimization of our framework, we employ the AdamW optimizer with a learning rate of  $1 \times 10^{-5}$ . The weights of the ID Encoder [6], Variational Autoencoder [25] from Stable Video Diffusion [2] and the blocks of DiNOv2 [38] are fixed. In the motion memory bank, we

Table 1. **Quantitative results on  $512 \times 512$  test images.** LMD multiplied by  $10^{-3}$ , AED multiplied by  $10^{-2}$ , APD multiplied by  $10^{-3}$  and Identity Similarity multiplied by  $10^{-1}$ .  $\uparrow$  indicates higher is better.  $\downarrow$  indicates lower is better. The best results are in bold.

Method	Self Reenactment						Cross Reenactment					
	LMD $\downarrow$	FID-VID $\downarrow$	FVD $\downarrow$	PSNR $\uparrow$	SSIM $\uparrow$	LPIPS $\downarrow$	AED $\downarrow$	APD $\downarrow$	Identity $\uparrow$ Similarity	Facial $\uparrow$ Movements	Video $\uparrow$ Quality	Temporal $\uparrow$ Smoothness
LivePortrait [14]	9.14	82.71	483.38	31.41	0.72	0.22	26.83	26.97	8.71	3.00	4.11	4.06
AniPortrait [53]	6.67	81.90	430.24	30.54	0.67	0.27	22.42	21.32	7.95	3.83	4.00	3.81
FollowYE [35]	5.63	77.15	417.53	30.84	0.68	0.25	20.06	20.95	8.18	4.11	4.23	3.33
X-Portrait [55]	6.23	82.93	416.41	30.81	0.71	0.19	20.66	20.39	8.03	3.88	3.73	3.49
HunyuanPortrait (Ours)	<b>2.02</b>	<b>75.81</b>	<b>333.48</b>	<b>32.98</b>	<b>0.81</b>	<b>0.11</b>	<b>19.45</b>	<b>19.20</b>	<b>8.87</b>	<b>4.55</b>	<b>4.69</b>	<b>4.61</b>

incorporate 64 learnable motion memories, each with a dimension of 768, which share parameters across the various blocks. They are initialized using a scaled normal distribution, where each element is sampled from  $\mathcal{N}(0, \frac{1}{\sqrt{\text{hidden\_dim}}})$ . To ensure stability, we apply gradient norm clipping at a value of 0.99. During inference, we employ the DDIM sampler [45] and set the scale of classifier-free guidance [17] to 2.0 for our experiment. The framework is trained on 128 NVIDIA A100 GPUs for three days.

## 4.2. Metrics

We employ both qualitative and quantitative analyses to assess the generated video quality and motion accuracy of our portrait animation results. For self-reenactment, we utilize the Fréchet Inception Distance (FID) [16], the Fréchet Video Distance (FVD) [48], Peak Signal-to-Noise Ratio (PSNR), Structural Similarity Index (SSIM) [52], Learned Perceptual Image Patch Similarity (LPIPS) [65] and the Landmark Mean Distances (LMD) [33]. For cross-reenactment, we utilize Average Expression Distance (AED) [44], Average Pose Distance (APD) [44] and the ArcFace Score [6] as the identity (ID) similarity. Detailed descriptions of these metrics are provided in *supplementary materials*. Considering the absence of ground truth and the significant error between current evaluation methods and human perception, we combine the results of user studies that evaluates cross-reenactment from three additional dimensions: facial movements, video quality, and temporal smoothness. The facial movements encompass not only facial expressions but also the overall orientation of the generated portrait head. The quality of the video and its temporal smoothness are primarily assessed by the clarity of the video and the smoothness of the transitions between frames. For evaluation, we utilize source images and driving videos from two prominent datasets [5, 54]. This experiment aims to evaluate the model’s ability to transfer expressions and movements from one subject to another while preserving the identity of the source portrait.

## 4.3. Quantitative and Qualitative Analysis

As shown in Table 1, our method attains the lowest FID-VID (average FID of frames in videos) and FVD, with a

significant advantage when compared to the previously top-performing method, which underscores the superior capability of HunyuanPortrait. We also find that non-diffusion-based methods have much lower generation quality compared to diffusion-based methods. Although the video resolution is the same, the generated portrait details have significant differences. In more challenging cross-reenactment scenarios, our approach demonstrates strong generalization capabilities, leading to substantial improvements across all metrics. This fully demonstrates the advantage of our method, as cross-reenactment is much more difficult than self-reenactment and is closer to real-life application scenarios. The warping-based method LivePortrait struggles to accurately model overall head movement, resulting in generated portraits that exhibit minimal variation in head pose relative to the reference image. Compared with other methods, our method has stronger ID similarity, facial dynamic generation ability, video quality, and temporal smoothness. Our method employs implicit motion representation rather than explicit facial keypoints to control the generation of facial expressions. Our method further takes into account the intensity of motion, the ability to perceive identity, and complementary information based on temporal context. This approach mitigates identity distortion caused by variations in facial geometries and effectively captures dynamic facial details that explicit keypoints cannot represent. Meanwhile, since our method is based on stable video diffusion, the generated results are smoother compared to previous image-based diffusion methods and have higher video quality. These enhancements highlight the superior accuracy and fidelity of our method in capturing fine-grained details, affirming its efficacy in synthesizing realistic portrait motions. Furthermore, due to the lack of open-source training code, combined with the challenges related to their motion module and the frame rate of the videos, FollowYourEmoji and X-Portrait shows suboptimal performance in terms of temporal smoothness. Our method remains unaffected by variations in frame rate.

## 4.4. Visualization

As illustrated in Figure 4, our method can capture more detailed and consistent portrait movements with the driv-



Figure 4. Qualitative comparisons of self-reenactment and cross-reenactment with state-of-the-art methods.

ing video. For self-reenactment, our method generates results that enable more detailed capture of facial dynamics, including eye gaze direction, eye rotation, and lip synchronization. In addition, our method can also achieve tracking of the overall rotation of the head, which cannot be achieved by previous top-performing warping-based method LivePortrait, such as LivePortrait. Current state-of-the-art diffusion-based methods have significant defects in maintaining the portrait’s identity and facial shape due to the deviation of predicted keypoints during head rotation. In contrast, our method effectively preserves the identity of the portrait and captures intricate facial dynamics. Previous methods are influenced by the differences in facial geometries between the driving video and the reference image,

leading to substantial challenges in preserving the identity of the generated video. This is a result of inadequate disentanglement of their appearance features and facial dynamics. These issues result in problems such as blurry videos and distorted portraits. Our framework effectively addresses the disentanglement of the two key elements involved in portrait animation, thereby demonstrating a strong generalization ability, as shown in Figure 4. The diffusion-based method exhibits superior generation quality; however, discrepancies in facial keypoints due to variations in facial shape, combined with the limited ability of these keypoints to accurately capture dynamic facial details, make the previous state-of-the-art method less effective than ours in generating features such as facial geometry, eye gaze direc-





Figure 5. Qualitative ablation studies of different components.

tion, and lip synchronization in portraits. Due to variations in facial shapes, methods that rely on explicit keypoints are influenced by the facial characteristics of individuals in the driving video. This leads to insufficient separation between motion and identity. Furthermore, since their approach utilizes the image generation model Stable Diffusion as its foundation, it also exhibits inferior performance compared to ours in terms of temporal smoothness. Building upon stable video diffusion and utilizing our meticulously designed fine-grained feature extractors, our method exhibits exceptional performance in identity preservation, video quality enhancement, and the capture of subtle facial movements, resulting in more vivid and smoother generated videos.

#### 4.5. Ablation Study

**Effect of Motion Memory Bank.** We validate the effectiveness of the motion memory bank. As shown in Table 2, the incorporation of the motion memory bank results in higher-quality videos, demonstrating improvements in FID-VID and FVD, as well as enhanced facial movements. We also observe an improvement in smoothness. Through the utilization of motion memories, our methodology demonstrates context-based perception capabilities, thereby enhancing motion features in the presence of ambiguous information. By integrating memories with information from preceding and subsequent frames, the memory bank can provide more detailed information into facial dynamics. As illustrated in Figure 5, the forehead wrinkles associated with the elevation of the eyes become more pronounced, when the character’s eyebrows are raised.

**Effect of Intensity-Aware Motion Encoder (IAME).** We confirm the significant role of the intensity-aware motion encoder. As illustrated in Table 2, the incorporation of this

Table 2. Ablation study to validate the effectiveness of different components. LMD (Landmark Mean Distance) multiplied by  $10^{-3}$  and Identity Similarity multiplied by  $10^{-1}$ .

Setting	Identity ↑ Similarity	FID-VID ↓	FVD ↓	LMD ↓
HunyuanPortrait	8.87	75.81	333.48	2.02
- Memory Bank	8.75	78.43	361.94	2.78
- IAME	8.63	80.79	385.43	4.01
- ID Features	8.21	75.03	330.12	1.98
- IMAdapter	8.09	77.14	352.67	2.54

component, in contrast to the direct utilization of coarse motion features derived from the pre-trained motion encoder [8], offers critical guidance and intricate details regarding the facial dynamics associated with portrait motions. This enhancement significantly elevates the overall quality of the generated video, evidenced by an improvement in FID-VID, FVD, and ID similarity. As illustrated in Figure 5, the absence of feature refinement in the IAME may result in inaccuracies in the micro-expressions of the characters, including the direction of their gaze. Furthermore, the intricate details of the face are neglected.

**Effect of ID features and IMAdapter.** To validate the effectiveness of the IMAdapter, we first remove the ID features from the IMAdapter, leaving only multiple convolution kernels for low-rank feature processing. As shown in Table 2 and Figure 5, the ablation results demonstrate that incorporating ID features is critical in enhancing the model’s ID consistency ability. We further remove IMAdapter from the appearance extractor’s blocks. As demonstrated in Figure 5, the incorporation of IMAdapter provides more fine-grained features related to facial texture, geometry, and other facial characteristics.

#### 5. Conclusion

In this paper, we present an enhanced portrait animation framework that addresses the limitations of previous approaches. Our model leverages implicit representations with stable video diffusion to achieve temporal consistency and precise control over facial dynamics. The proposed model demonstrates significant improvements in the overall quality and temporal consistency of generated videos, allowing for more natural and lifelike animations. We offer a robust framework for generating high-quality, controllable animations, which achieve high disentanglement. Our method not only enhances the visual experience but also opens up possibilities for immersive content creation. With continued research and development, this approach holds great potential for applications in virtual reality, gaming, and human-computer interaction. However, as with any technology that generates realistic human likenesses, future work should develop safeguards to ensure responsible use.



## References

- [1] Andreas Blattmann, Tim Dockhorn, Sumith Kulal, Daniel Mendelevitch, Maciej Kilian, Dominik Lorenz, Yam Levi, Zion English, Vikram Voleti, Adam Letts, et al. Stable video diffusion: Scaling latent video diffusion models to large datasets. *arXiv preprint arXiv:2311.15127*, 2023. 4
- [2] Andreas Blattmann, Tim Dockhorn, Sumith Kulal, Daniel Mendelevitch, Maciej Kilian, Dominik Lorenz, Yam Levi, Zion English, Vikram Voleti, Adam Letts, et al. Stable video diffusion: Scaling latent video diffusion models to large datasets. *arXiv preprint arXiv:2311.15127*, 2023. 5
- [3] Zhiyuan Chen, Jiajiong Cao, Zhiquan Chen, Yuming Li, and Chenguang Ma. Echomimic: Lifelike audio-driven portrait animations through editable landmark conditions. *arXiv preprint arXiv:2407.08136*, 2024. 1, 2
- [4] Kun Cheng, Xiaodong Cun, Yong Zhang, Menghan Xia, Fei Yin, Mingrui Zhu, Xuan Wang, Jue Wang, and Nannan Wang. Videoretalking: Audio-based lip synchronization for talking head video editing in the wild. In *SIGGRAPH Asia 2022*, pages 1–9, 2022. 1
- [5] Joon Son Chung, Arsha Nagrani, and Andrew Zisserman. Voxceleb2: Deep speaker recognition. *arXiv preprint arXiv:1806.05622*, 2018. 5, 6
- [6] Jiankang Deng, Jia Guo, Niannan Xue, and Stefanos Zafeiriou. Arcface: Additive angular margin loss for deep face recognition. In *Proceedings of the IEEE/CVF conference on computer vision and pattern recognition*, pages 4690–4699, 2019. 2, 4, 5, 6, 12
- [7] Michail Christos Doukas, Stefanos Zafeiriou, and Viktoriia Sharmanska. Headgan: One-shot neural head synthesis and editing, 2021. 1, 2
- [8] Nikita Drobyshev, Jenya Chelishev, Taras Khakhulin, Aleksei Ivakhnenko, Victor Lempitsky, and Egor Zakharov. Megaportraits: One-shot megapixel neural head avatars. In *Proceedings of the 30th ACM International Conference on Multimedia*, pages 2663–2671, 2022. 4, 8, 13
- [9] Nikita Drobyshev, Jenya Chelishev, Taras Khakhulin, Aleksei Ivakhnenko, Victor Lempitsky, and Egor Zakharov. Megaportraits: One-shot megapixel neural head avatars, 2023. 2
- [10] Stefan Elfving, Eiji Uchibe, and Kenji Doya. Sigmoid-weighted linear units for neural network function approximation in reinforcement learning. *Neural networks*, 107:3–11, 2018. 13
- [11] Ian Goodfellow, Jean Pouget-Abadie, Mehdi Mirza, Bing Xu, David Warde-Farley, Sherjil Ozair, Aaron Courville, and Yoshua Bengio. Generative adversarial networks. *Communications of the ACM*, 63(11):139–144, 2020. 1
- [12] Yuming Gu, Hongyi Xu, You Xie, Guoxian Song, Yichun Shi, Di Chang, Jing Yang, and Linjie Luo. Diffportrait3d: Controllable diffusion for zero-shot portrait view synthesis. In *Proceedings of the IEEE/CVF Conference on Computer Vision and Pattern Recognition*, pages 10456–10465, 2024. 1, 12
- [13] Hanzhong Guo, Hongwei Yi, Daquan Zhou, Alexander William Bergman, Michael Lingelbach, and Yizhou Yu. Real-time one-step diffusion-based expressive portrait videos generation. *arXiv preprint arXiv:2412.13479*, 2024. 2
- [14] Jianzhu Guo, Dingyun Zhang, Xiaoqiang Liu, Zhizhou Zhong, Yuan Zhang, Pengfei Wan, and Di Zhang. Liveportrait: Efficient portrait animation with stitching and retargeting control. *arXiv preprint arXiv:2407.03168*, 2024. 2, 6
- [15] Yuwei Guo, Ceyuan Yang, Anyi Rao, Zhengyang Liang, Yaohui Wang, Yu Qiao, Maneesh Agrawala, Dahua Lin, and Bo Dai. Animatediff: Animate your personalized text-to-image diffusion models without specific tuning. In *The Twelfth International Conference on Learning Representations*, 2024. 2
- [16] Martin Heusel, Hubert Ramsauer, Thomas Unterthiner, Bernhard Nessler, and Sepp Hochreiter. Gans trained by a two time-scale update rule converge to a local nash equilibrium. *Advances in neural information processing systems*, 30, 2017. 6, 12
- [17] Jonathan Ho and Tim Salimans. Classifier-free diffusion guidance. *arXiv preprint arXiv:2207.12598*, 2022. 6
- [18] Fa-Ting Hong and Dan Xu. Implicit identity representation conditioned memory compensation network for talking head video generation. In *Proceedings of the IEEE/CVF International Conference on Computer Vision*, pages 23062–23072, 2023. 2
- [19] Fa-Ting Hong, Li Shen, and Dan Xu. Dagan++: Depth-aware generative adversarial network for talking head video generation. *IEEE Transactions on Pattern Analysis and Machine Intelligence*, 2023. 2
- [20] Li Hu. Animate anyone: Consistent and controllable image-to-video synthesis for character animation. In *Proceedings of the IEEE/CVF Conference on Computer Vision and Pattern Recognition*, pages 8153–8163, 2024. 5
- [21] Xianliang Huang, Jiajie Gou, Shuhang Chen, Zhizhou Zhong, Jihong Guan, and Shuigeng Zhou. Iddr-ngp: Incorporating detectors for distractors removal with instant neural radiance field. In *Proceedings of the 31st ACM International Conference on Multimedia*, pages 1343–1351, 2023. 2
- [22] Xiaoyu Jin, Zunnan Xu, Mingwen Ou, and Wenming Yang. Alignment is all you need: A training-free augmentation strategy for pose-guided video generation. *arXiv preprint arXiv:2408.16506*, 2024. 2
- [23] Taras Khakhulin, Vanessa Sklyarova, Victor Lempitsky, and Egor Zakharov. Realistic one-shot mesh-based head avatars. In *European Conference on Computer Vision*, pages 345–362. Springer, 2022. 2
- [24] Diederik P Kingma and Max Welling. Auto-encoding variational bayes. *arXiv preprint arXiv:1312.6114*, 2013. 3
- [25] Diederik P Kingma and Max Welling. Auto-encoding variational bayes. *arXiv preprint arXiv:1312.6114*, 2013. 5
- [26] Weijie Kong, Qi Tian, Zijian Zhang, Rox Min, Zuozhuo Dai, Jin Zhou, Jiangfeng Xiong, Xin Li, Bo Wu, Jianwei Zhang, et al. Hunyuanvideo: A systematic framework for large video generative models. *arXiv preprint arXiv:2412.03603*, 2024. 2
- [27] Hongxiang Li, Meng Cao, Xuxin Cheng, Yaowei Li, Zhihong Zhu, and Yuexian Zou. G2l: Semantically aligned and uniform video grounding via geodesic and game theory. In

*Proceedings of the IEEE/CVF International Conference on Computer Vision*, pages 12032–12042, 2023. 2

- [28] Hongxiang Li, Yaowei Li, Yuhang Yang, Junjie Cao, Zhihong Zhu, Xuxin Cheng, and Long Chen. Dispose: Disentangling pose guidance for controllable human image animation. *arXiv preprint arXiv:2412.09349*, 2024. 2
- [29] Ronghui Li, Junfan Zhao, Yachao Zhang, Mingyang Su, Zeping Ren, Han Zhang, Yansong Tang, and Xiu Li. Finedance: A fine-grained choreography dataset for 3d full body dance generation. In *Proceedings of the IEEE/CVF International Conference on Computer Vision*, pages 10234–10243, 2023. 1
- [30] Ronghui Li, Hongwen Zhang, Yachao Zhang, Yuxiang Zhang, Youliang Zhang, Jie Guo, Yan Zhang, Xiu Li, and Yebin Liu. Lodge++: High-quality and long dance generation with vivid choreography patterns. *arXiv preprint arXiv:2410.20389*, 2024.
- [31] Ronghui Li, Yuxiang Zhang, Yachao Zhang, Hongwen Zhang, Jie Guo, Yan Zhang, Yebin Liu, and Xiu Li. Lodge: A coarse to fine diffusion network for long dance generation guided by the characteristic dance primitives. In *Proceedings of the IEEE/CVF Conference on Computer Vision and Pattern Recognition*, pages 1524–1534, 2024. 1
- [32] Gang LIU, Xin CHEN, and Zhixiang GAO. A novel double-tail generative adversarial network for fast photo animation. *IEICE Transactions on Information and Systems*, E107.D(1): 72–82, 2024. 5
- [33] Camillo Lugaresi, Jiuqiang Tang, Hadon Nash, Chris McClanahan, Esha Uboweja, Michael Hays, Fan Zhang, Chuoling Chang, Ming Guang Yong, Juhyun Lee, et al. Mediapipe: A framework for building perception pipelines. *arXiv preprint arXiv:1906.08172*, 2019. 6, 12
- [34] Yue Ma, Yingqing He, Xiaodong Cun, Xintao Wang, Siran Chen, Xiu Li, and Qifeng Chen. Follow your pose: Pose-guided text-to-video generation using pose-free videos. In *Proceedings of the AAAI Conference on Artificial Intelligence*, pages 4117–4125, 2024. 4
- [35] Yue Ma, Hongyu Liu, Hongfa Wang, Heng Pan, Yingqing He, Junkun Yuan, Ailing Zeng, Chengfei Cai, Heung-Yeung Shum, Wei Liu, et al. Follow-your-emoji: Fine-controllable and expressive freestyle portrait animation. *arXiv preprint arXiv:2406.01900*, 2024. 6
- [36] Yuxi Mi, Zhizhou Zhong, Yuge Huang, Jiazhen Ji, Jianqing Xu, Jun Wang, Shaoming Wang, Shouhong Ding, and Shuigeng Zhou. Privacy-preserving face recognition using trainable feature subtraction. In *Proceedings of the IEEE/CVF Conference on Computer Vision and Pattern Recognition*, pages 297–307, 2024. 2
- [37] Yuval Nirkin, Yosi Keller, and Tal Hassner. Fsgan: Subject agnostic face swapping and reenactment. In *Proceedings of the IEEE/CVF international conference on computer vision*, pages 7184–7193, 2019. 1
- [38] Maxime Oquab, Timothée Darcet, Théo Moutakanni, Huy Vo, Marc Szafraniec, Vasil Khalidov, Pierre Fernandez, Daniel Haziza, Francisco Massa, Alaaeldin El-Nouby, et al. Dinov2: Learning robust visual features without supervision. *arXiv preprint arXiv:2304.07193*, 2023. 2, 4, 5
- [39] Bohao Peng, Jian Wang, Yuechen Zhang, Wenbo Li, Ming-Chang Yang, and Jiaya Jia. Controlnext: Powerful and efficient control for image and video generation. *arXiv preprint arXiv:2408.06070*, 2024. 2, 5
- [40] George Retsinas, Panagiotis P Filntisis, Radek Danecek, Victoria F Abrevaya, Anastasios Roussos, Timo Bolkart, and Petros Maragos. 3d facial expressions through analysis-by-neural-synthesis. In *CVPR*, 2024. 12
- [41] Robin Rombach, Andreas Blattmann, Dominik Lorenz, Patrick Esser, and Björn Ommer. High-resolution image synthesis with latent diffusion models, 2021. 2, 3
- [42] Olaf Ronneberger, Philipp Fischer, and Thomas Brox. U-net: Convolutional networks for biomedical image segmentation. In *Medical image computing and computer-assisted intervention—MICCAI 2015: 18th international conference, Munich, Germany, October 5-9, 2015, proceedings, part III 18*, pages 234–241. Springer, 2015. 3
- [43] Aliaksandr Siarohin, Stéphane Lathuilière, Sergey Tulyakov, Elisa Ricci, and Nicu Sebe. First order motion model for image animation. *Advances in neural information processing systems*, 32, 2019. 1
- [44] Aliaksandr Siarohin, Stéphane Lathuilière, Sergey Tulyakov, Elisa Ricci, and Nicu Sebe. First order motion model for image animation. In *Advances in Neural Information Processing Systems*, 2019. 2, 6, 12
- [45] Jiaming Song, Chenlin Meng, and Stefano Ermon. Denoising diffusion implicit models. *arXiv preprint arXiv:2010.02502*, 2020. 6
- [46] Jiale Tao, Shuhang Gu, Wen Li, and Lixin Duan. Learning motion refinement for unsupervised face animation. *Advances in Neural Information Processing Systems*, 36, 2024. 2
- [47] Jiayuan TIAN, Yanling LONG, Hong YANG, Huifang WU, Peng XUE, and Zhongqing JIANG. Cues of eye region and their effects on face-personality perception. *Advances in Psychological Science*, 30(12):2735, 2022. 2
- [48] Thomas Unterthiner, Sjoerd van Steenkiste, Karol Kurach, Raphaël Marinier, Marcin Michalski, and Sylvain Gelly. Fvd: A new metric for video generation. 2019. 6, 12
- [49] Ashish Vaswani, Noam Shazeer, Niki Parmar, Jakob Uszkoreit, Llion Jones, Aidan N Gomez, Łukasz Kaiser, and Illia Polosukhin. Attention is all you need. *Advances in Neural Information Processing Systems*, 30, 2017. 4
- [50] Cong Wang, Kuan Tian, Jun Zhang, Yonghang Guan, Feng Luo, Fei Shen, Zhiwei Jiang, Qing Gu, Xiao Han, and Wei Yang. V-express: Conditional dropout for progressive training of portrait video generation. *arXiv preprint arXiv:2406.02511*, 2024. 1, 2, 5
- [51] Suzhen Wang, Lincheng Li, Yu Ding, and Xin Yu. One-shot talking face generation from single-speaker audio-visual correlation learning. In *AAAI Conference on Artificial Intelligence*, pages 2531–2539, 2022. 2
- [52] Zhou Wang, Alan C Bovik, Hamid R Sheikh, and Eero P Simoncelli. Image quality assessment: from error visibility to structural similarity. *IEEE transactions on image processing*, 13(4):600–612, 2004. 6, 12

- [53] Huawei Wei, Zejun Yang, and Zhisheng Wang. Aniportrait: Audio-driven synthesis of photorealistic portrait animations, 2024. [2](#), [4](#), [6](#)
- [54] Liangbin Xie, Xintao Wang, Honglun Zhang, Chao Dong, and Ying Shan. Vfhq: A high-quality dataset and benchmark for video face super-resolution. In *Proceedings of the IEEE/CVF Conference on Computer Vision and Pattern Recognition*, pages 657–666, 2022. [5](#), [6](#)
- [55] You Xie, Hongyi Xu, Guoxian Song, Chao Wang, Yichun Shi, and Linjie Luo. X-portrait: Expressive portrait animation with hierarchical motion attention. In *ACM SIGGRAPH 2024 Conference Papers*, pages 1–11, 2024. [2](#), [6](#), [12](#)
- [56] Jingjing Xu, Xu Sun, Zhiyuan Zhang, Guangxiang Zhao, and Junyang Lin. Understanding and improving layer normalization. *Advances in neural information processing systems*, 32, 2019. [4](#)
- [57] Sicheng Xu, Guojun Chen, Yu-Xiao Guo, Jiaolong Yang, Chong Li, Zhenyu Zang, Yizhong Zhang, Xin Tong, and Baining Guo. Vasa-1: Lifelike audio-driven talking faces generated in real time. *arXiv preprint arXiv:2404.10667*, 2024. [2](#)
- [58] Zunnan Xu, Yukang Lin, Haonan Han, Sicheng Yang, Ronghui Li, Yachao Zhang, and Xiu Li. Mambatalk: Efficient holistic gesture synthesis with selective state space models. In *The Thirty-eighth Annual Conference on Neural Information Processing Systems*, 2024. [1](#)
- [59] Shurong Yang, Huadong Li, Juhao Wu, Minhao Jing, Linze Li, Renhe Ji, Jiajun Liang, and Haoqiang Fan. Megactor: Harness the power of raw video for vivid portrait animation. *arXiv preprint arXiv:2405.20851*, 2024. [2](#)
- [60] Zhendong Yang, Ailing Zeng, Chun Yuan, and Yu Li. Effective whole-body pose estimation with two-stages distillation. In *Proceedings of the IEEE/CVF International Conference on Computer Vision*, pages 4210–4220, 2023. [5](#)
- [61] Hu Ye, Jun Zhang, Sibao Liu, Xiao Han, and Wei Yang. Ip-adapter: Text compatible image prompt adapter for text-to-image diffusion models. *arXiv preprint arXiv:2308.06721*, 2023. [4](#)
- [62] Fei Yin, Yong Zhang, Xiaodong Cun, Mingdeng Cao, Yanbo Fan, Xuan Wang, Qingyan Bai, Baoyuan Wu, Jue Wang, and Yujiu Yang. Styleheat: One-shot high-resolution editable talking face generation via pre-trained stylegan. In *European Conference on Computer Vision*, pages 85–101, 2022. [2](#)
- [63] Wangbo Yu, Yanbo Fan, Yong Zhang, Xuan Wang, Fei Yin, Yunpeng Bai, Yan-Pei Cao, Ying Shan, Yang Wu, Zhongqian Sun, and Baoyuan Wu. Nofa: Nerf-based one-shot facial avatar reconstruction, 2023. [2](#)
- [64] Bowen Zhang, Chenyang Qi, Pan Zhang, Bo Zhang, Hsiang-Tao Wu, Dong Chen, Qifeng Chen, Yong Wang, and Fang Wen. Metaportrait: Identity-preserving talking head generation with fast personalized adaptation. In *Proceedings of the IEEE/CVF Conference on Computer Vision and Pattern Recognition*, pages 22096–22105, 2023. [1](#), [2](#)
- [65] Richard Zhang, Phillip Isola, Alexei A Efros, Eli Shechtman, and Oliver Wang. The unreasonable effectiveness of deep features as a perceptual metric. In *Proceedings of the IEEE conference on computer vision and pattern recognition*, pages 586–595, 2018. [6](#), [12](#)
- [66] Yang Zhang, Jiaxi Gu, Li-Wen Wang, Han Wang, Junqi Cheng, Yuefeng Zhu, and Fangyuan Zou. Mimicmotion: High-quality human motion video generation with confidence-aware pose guidance. *arXiv preprint arXiv:2406.19680*, 2024. [2](#), [5](#)
- [67] Zhimeng Zhang, Lincheng Li, Yu Ding, and Changjie Fan. Flow-guided one-shot talking face generation with a high-resolution audio-visual dataset. In *Proceedings of the IEEE/CVF Conference on Computer Vision and Pattern Recognition*, pages 3661–3670, 2021. [5](#)
- [68] Jian Zhao and Hui Zhang. Thin-plate spline motion model for image animation. In *Proceedings of the IEEE/CVF Conference on Computer Vision and Pattern Recognition*, pages 3657–3666, 2022. [2](#)
- [69] Longtao Zheng, Yifan Zhang, Hanzhong Guo, Jiachun Pan, Zhenxiong Tan, Jiahao Lu, Chuanxin Tang, Bo An, and Shuicheng Yan. Memo: Memory-guided diffusion for expressive talking video generation. *arXiv preprint arXiv:2412.04448*, 2024. [2](#)
- [70] Hao Zhu, Wayne Wu, Wentao Zhu, Liming Jiang, Siwei Tang, Li Zhang, Ziwei Liu, and Chen Change Loy. Celebv-hq: A large-scale video facial attributes dataset. In *European conference on computer vision*, pages 650–667. Springer, 2022. [5](#)

## A. Benchmark Metrics Details

We employ both qualitative and quantitative analyses to assess the generated video quality and motion accuracy of our portrait animation results. In evaluating self-reenactment, we consider multiple metrics: the Peak Signal-to-Noise Ratio (PSNR), the Structural Similarity Index (SSIM) [52], and the Learned Perceptual Image Patch Similarity (LPIPS) [65]. Specifically, for the LPIPS metric, we apply the AlexNet-based perceptual similarity measure LPIPS [65] to gauge the perceptual similarity between the generated animated images and the driving images. We also utilize the Fréchet Inception Distance (FID) [16] to assess image quality, the Fréchet Video Distance (FVD) [48] to evaluate temporal consistency, and the Landmark Mean Distances (LMD) to measure the accuracy of generated facial expressions. The landmarks are extracted using Mediapipe [33]. We compute the average Euclidean distance between the facial landmarks [33] of the reference and generated frames. Lower values indicate better geometric accuracy. FID [16] is utilized to measure the similarity in feature distribution between generated and real images, employing Inception-v3 features. Lower scores indicate better perceptual quality. Additionally, the FVD is used to evaluate temporal coherence through features extracted from a pretrained network [48]. For cross-reenactment, we utilize the ArcFace Score [6] as the identity (ID) similarity metric between the generated frames and the reference image. For Average Expression Distance (AED) [44] and Average Pose Distance (APD) [44], we calculate the Manhattan distance of expression and pose parameters from SMIRK [40], with lower values indicating better expression and pose similarity.

## B. Discussions, Limitations and Future work

In this section, we make comparisons of our method on ID modules with X-Portrait [55] and DiffPortrait3D [12]. The ID modules share the common objective of preserving the identity of the reference portrait during the generation of new animations or views. However, each method employs distinct strategies to achieve this goal, leading to differences in implementation, training, and application focus.

Our method utilizes a fine-grained appearance extractor coupled with an ID-aware multi-scale adapter (IMAdapter). This design enables detailed modeling of identity and background information from the reference image, ensuring high-fidelity identity preservation in the generated animations. The IMAdapter incorporates multi-scale convolutions and cross-attention mechanisms, which enhance the model’s ability to capture intricate identity features and maintain their consistency across different frames and contexts. In contrast, X-Portrait’s ID module extracts appearance and background features from a single reference image, which are then concatenated into the UNet’s trans-

former blocks. This straightforward approach ensures consistent identity representation across generated frames but may not capture fine-grained details as effectively as our multi-scale architecture. X-Portrait focuses on expressive portrait animation, aiming to transfer facial expressions and head poses from driving videos to the reference portrait while maintaining identity similarity.

DiffPortrait3D adopts a different strategy by injecting appearance context from the reference image into the self-attention layers of a frozen UNet. This method effectively preserves identity across various rendering views but is primarily designed for 3D view synthesis rather than full animation. It leverages the generative power of pre-trained diffusion models to synthesize 3D-consistent novel views from as few as a single portrait.

For future work, we believe that exploring the synthesis of images from unknown perspectives to enhance identity retention capability is crucial. The current method has limitations in maintaining identity consistency from unknown perspectives after significant head rotation. The ID preservation design of DiffPortrait3D presents a potential improvement; however, it is still constrained by specific angles and cannot achieve the generation of unknown 360-degree views. We assert that enhancing the identity retention capability from unknown perspectives is a vital and feasible direction for improving the method proposed in this paper.

Besides, there are still several limitations with our method. Currently, our methodology is restricted to generating only the head and shoulder portions of portraits. We try to apply our method for generating full-body portraits that include hands; however, the results are unsatisfactory. The generated images of hands occasionally exhibit deformities and blurriness. This limitation stems from the inadequate representation of hand regions within the dataset, which hinders our ability to accurately render hand details. Future work can enhance our method by incorporating data that includes hand movements and improving the representation of hand features, thereby extending our approach to encompass full-body movements. Additionally, our approach is limited by the inherent constraints of the diffusion model. The significant computational costs impede the real-time applicability of our methods. Future work can accelerate the generation process through model distillation.

## C. More Implementation Details

### C.1. Appearance Extractor

For the input of the appearance extractor, we first resize the reference image to 256x256. We use the DiNOv2-Large with 4 register tokens as the appearance extractor, and fix the weights of its backbone during training. In the implementation of the IMAdapter, we first reduce the dimensionality of the features to 384 using linear layers. Subse-



quently, we employ convolutional kernels of varying scales (e.g.,  $1 \times 1$ ,  $3 \times 3$ ,  $5 \times 5$ ) for parallel processing and fuse these with ID features through a multi-head cross-attention mechanism. We set the number of heads for the multi-head cross-attention to 8.

## C.2. Motion Extractor

The motion extractor comprises a total of six blocks within the network, utilizing consistent network configurations. The dimensionality of the latent features is set at 768, with the attention mechanism employing eight heads. The activation function implemented is the Sigmoid Linear Unit (SiLU) [10]. The motion encoder is borrowed from Mega-Portrait [8]. We upgrade the architecture of the motion encoder from ResNet-18 to ResNet-50 to facilitate the pre-training of the motion encoder. After completing pre-training, the weights of this motion encoder is fixed and utilized for fine-tuning SVD.

## D. More Visualizations

As shown in Figure 6, we present additional visualization results under the self-reenactment and cross-reenactment setting to better demonstrate the decoupling capability of our method in terms of appearance and motion. In order to demonstrate the robust generalization of our method, we selected a variety of images and videos from different style domains, including Civitai <sup>\*</sup>, Bilibili <sup>†</sup>, and VFHQ <sup>‡</sup>, for demonstration purposes. To avoid copyright issues with driving videos, we first use a source image along with the original video to obtain the generated result. As illustrated in Figure 7, Figure 8 and Figure 9, we then utilize the generated results as the driving videos to animate other videos.

## E. Ethics Consideration

### E.1. User Study Details

In the user study, a total of 120 experienced participants are invited to take part. For each participant, we paid compensation that exceeded the local average hourly wage. We employ three metrics: Facial Movement, Video Quality, and Temporal Smoothness. For each metric, participants are presented with a video rated on a five-point scale. The grading options available to participants were as follows: Very Good (5), Good (4), Average (3), Poor (2), and Very Poor (1). As illustrated in Figure 10, the online evaluations are conducted using a well-structured website questionnaire. The questionnaire provides a comprehensive guideline, along with several example videos at the beginning. These example videos are not included in the rating

but serve to illustrate the quality of video generation and ensure consistency in the rating criteria among participants.

## E.2. Societal Impacts and Responsible AI

Our focus is on advancing the visual effects of virtual AI avatars to enhance their effectiveness for beneficial applications. It is essential to clarify that our research objectives are not intended to deceive or mislead. Like other content creation methods, our approach is not immune to potential misuse. We firmly oppose any misuse that could result in the creation of deceptive or harmful content through the impersonation of real individuals. Despite the risks of misuse, it’s important to highlight the substantial positive outcomes of our technology. These include promoting educational fairness, aiding those with communication difficulties, and offering companionship or therapeutic aid. The significance of our research is underscored by its potential to assist those in need. We are committed to the ethical progression of AI, with the goal of fostering human welfare. The output videos generated by our method still retain identifiable traces of the actual individuals they are based on. To mitigate the potential for abuse, we are developing a neural network-powered tool designed to differentiate between genuine and synthetic videos, which includes our synthetic talking face videos in the training dataset. We will keep the community updated on any advancements in our models.

---

<sup>\*</sup><https://civitai.com>

<sup>†</sup><https://bilibili.com>

<sup>‡</sup><https://liangbinxie.github.io/projects/vfhq>







Figure 7. More visualizations of animated portraits.





Figure 8. More visualizations of animated portraits.





Figure 9. More visualizations of animated portraits.

# Rate your score on these videos.

In this task you are presented with mutiple videos of animated virtual characters.

You will be asked to rate the videos based on three different criteria.

Please focus on head movements and the facial expressions of the characters.

You also need to pay attention to the quality and the temporal smoothness of video generation.

Please press play in order to start the videos. You need to watch videos at least once to be able to answer.

## Source Image | Driving Video | Generated Video



1. How similar are the characters' head movements and facial expressions in the generated video to those in the driving video in terms of authenticity and naturalness?

☐ Very Good    ☐ Good    ☐ Average    ☐ Poor    ☐ Very Poor

2. How would you rate the clarity and resolution of the videos? Consider sharpness, blurriness, detail in characters and movements, and any artifacts or distortions affecting visual quality.

☐ Very Good    ☐ Good    ☐ Average    ☐ Poor    ☐ Very Poor

3. How would you assess the fluidity and consistency of the characters' movements in the video? Consider frame transitions, and the naturalness of motion. Are there any delays or inconsistencies that disrupt continuity?

☐ Very Good    ☐ Good    ☐ Average    ☐ Poor    ☐ Very Poor

Next Video

Submit All

Figure 10. The screenshots of user study website for participants.